Turkish Journal of Physics

http://journals.tubitak.gov.tr/physics/

Research Article

Turk J Phys
(2019) 43: 138 – 146

doi:10.3906/fiz-1807-27

Theoretical description of the two-color photoelectron spectra process of hydrogen: comparison between TDSE calculation and Kroll and Watson approach

Souhaila CHADDOU[1,*], **Soumia CHQONDI**[1], **Abdelmalek TAOUTIOUI**[1], **Abdelkader MAKHOUTE**[1,2]

[1]Physics of Radiation and Laser-Matter Interactions, Faculty of Sciences, University of Moulay Ismail, Meknès, Morocco

[2]Faculty of Sciences, Free University of Brussels (ULB), Brussels, Belgium

Received: 12.07.2018 • **Accepted/Published Online:** 13.02.2019 • **Final Version:** 08.04.2019

Abstract: We present a theoretical study of the main characteristics of two-color photoionization of hydrogen atoms by short strong laser pulses. Our numerical approach is performed by numerically solving the time-dependent Schrödinger equation for a hydrogen atom interacting with Ti:sapphire laser radiation combined with its 15th harmonic. The energy spectra obtained by the direct numerical solution of the Schrödinger equation are compared with those given by the Kroll and Watson perturbative approach. This comparison allows us to check the reliability of the latter approximation.

Key words: Time-dependent Schrödinger equation, above-threshold ionization, two-color photoionization, Kroll and Watson approach, infrared radiation, harmonic radiation

1. Introduction

During recent years, the availability of increasingly more powerful lasers has stimulated considerable interest in the study of multiphoton phenomena. In particular, the multiphoton ionization process [1], tunneling ionization [2], above-threshold ionization (ATI) process [3, 4], and high-order harmonics [5–7] have attracted a great deal of attention after being exploited in the developement of new sources of coherent radiation. Following the discovery of these new sources of light it was convenient to study the dynamics of atomic systems in interaction with two short strong laser pulses: ionization by harmonic photons in the presence of the generating external laser field.

We propose to study two-color IR-UV multiphoton ionization processes simultaneously using the fundamental of a strong IR laser and one of its higher UV harmonics, the latter having a frequency high enough to ionize the atom, through single-photon absorption. In such a condition, ionization can result from the absorption of the high-frequency photon together with the exchange of one or several infrared laser photon. In this context, numerous theoretical and experimental results [8–12] have been published by analyzing the energy spectra of the obtained photoelectrons. The two-color photoionization spectra reveal the existence of a certain number of energy peaks situated symmetrically around the harmonic peak. These latter peaks are known as the side-band peaks, related to the corresponding harmonic peak. They are the signature of an exchange of many infrared photons by absorption or stimulated emission with the IR laser. Our work consists of numerically solving the time-dependent Schrödinger equation (TDSE) defining the interaction of a hydrogen atom with short strong laser pulses. The simulation was carried out via an ab initio numerical resolution of the

*Correspondence: souhasmp@live.fr

TDSE for a three-dimensional (3D) hydrogen atom. For that, we chose the grid method, which consists of the discretization of the quantities that we want to propagate both in space and in time, i.e. where the partial derivatives in space are approximated by the method of finite difference to three points. The propagation over time of the wave function is assured by another integration method similar to that used by Kulander [13]. This is the Peaceman–Rachford method [14, 15] coupled with an inverse iteration procedure. Once the final wave function is obtained, a spectral analysis of the ejected electron based on the use of the window operator is performed. Our aim is to compare the numerical results calculated through the TDSE with those obtained by the semiclassical treatment theory provided by Kroll and Watson in 1973 [16] for calculating the differential cross-section of the electron scattering process in the presence of a laser field. The present work is structured as follows. In Section 2, we review the main steps to numerically solve the TDSE using the grid method and give a brief summary of the Kroll and Watson approach (KWA). Section 3 is dedicated to the presentation and discussion of the obtained results. Finally, in Section 4, we give the conclusions of our paper. Atomic units ($\hbar = m = e = 1$) are used throughout the derivation.

2. Theoretical approach

2.1. Numerical solution of time-dependent Schrödinger equation

The dynamics of an atom in a strong laser field are known by solving the TDSE:

$$i\frac{\partial}{\partial t}\psi(\vec{r},t) = H(\vec{r},t)\psi(\vec{r},t). \tag{2.1}$$

The total Hamiltonian $H(\vec{r},t)$ of the system can be decomposed as

$$H = H_0 + H_{int}(t), \tag{2.2}$$

where H_0 is the time-independent Hamiltonian of the target atom. For hydrogen, it can be written as

$$H_0 = -\frac{1}{2}\Delta - \frac{1}{r}\,. \tag{2.3}$$

The laser–atom interaction is considered within the dipole approximation where the interaction Hamiltonian is given in the length gauge by

$$H_{int} = \vec{E}(t).\vec{r}\,. \tag{2.4}$$

For a linearly polarized laser pulse (along the z axis), the electric field is chosen as

$$\vec{E}(t) = f(t)\big(E_{IR}\sin(\omega_{IR}t) + E_{H_{15}}sin(15\,\omega_{IR}t)\big)\vec{e_z}, \tag{2.5}$$

where $\vec{e_z}$ represents the polarization unit vector and the constants $E_{H_{15}}$ and E_{IR} are the amplitude of the harmonic field and the infrared field at the center of the laser pulse, respectively. The envelope $f(t)$ has the following trapezoidal form:

$$f(t) = \begin{cases} t/5T_{IR} & 0 \le t < 5T_{IR} \\ 1 & 5T_{IR} \le t < 35T_{IR} \\ 8 - t/5T_{IR} & 35T_{IR} \le t < 40T_{IR}\,, \end{cases} \tag{2.6}$$

where the pulse duration is fixed to 40 optical cycles of the infrared laser of period T_{IR}.

The TDSE in Eq. (2.1) is then written in spherical coordinates as follows:

$$i\frac{\partial}{\partial t}\psi(r,\theta,\phi,t) = \left[-\frac{1}{2r^2}\frac{\partial}{\partial r}\left(r^2\frac{\partial}{\partial r}\right) + \frac{L^2}{2r^2} - \frac{1}{r} + \vec{E}(t).\vec{r}\right]\psi(r,\theta,\phi,t). \tag{2.7}$$

The lasers are polarized linearly, which conserves the magnetic quantum number. Therefore, the unknown wave function ψ can be expanded in terms of spherical harmonics as

$$\psi(r,\theta,\phi,t) = \sum_{\ell=0}^{\ell_{max}} \frac{R_\ell(r,t)}{r} Y_{\ell,0}(\theta,\phi), \tag{2.8}$$

where the magnetic quantum number m is chosen arbitrarily equal to zero and ℓ_{max} is the maximum number of the angular momentum ℓ.

By substitution of the latter expansion in Eq. (2.7), we find

$$i\frac{\partial}{\partial t}R_\ell(r,t) = \left[-\frac{1}{2}\frac{d^2}{dr^2} - \frac{1}{r} + \frac{\ell(\ell+1)}{2r^2} + rE(t) < Y_{\ell',0} \mid \cos\theta \mid Y_{\ell,0} > \right] R_\ell(r,t). \tag{2.9}$$

The elements of the cosine matrix in the angular momentum basis are given by

$$< Y_{\ell',0} \mid \cos\theta \mid Y_{\ell,0} >= a_\ell \delta_{\ell',\ell+1} + a_{\ell-1}\delta_{\ell',\ell-1}\ , \tag{2.10}$$

where coefficients a_ℓ are given by

$$a_\ell = \frac{(\ell+1)}{\sqrt{(2\ell+1)(2\ell+3)}}. \tag{2.11}$$

In the grid method, the kinetic energy operator in Eq. (2.9) is discretized using the three-point finite difference method used in the [13]:

$$\begin{aligned} i\frac{\partial}{\partial t}R_{j,\ell}(t) = &-\frac{1}{2(\Delta r)^2}\left[c_{j-1}R_{j-1,\ell}(t) - 2d_jR_{j,\ell}(t) + c_jR_{j+1,\ell}(t)\right] + \left(\frac{\ell(\ell+1)}{2r_j^2} - \frac{1}{r_j}\right)R_{j,\ell}(t) \\ &+ E(t)r_jf(t)\left[a_\ell R_{j,\ell+1}(r,t) + a_{\ell-1}R_{j,\ell-1}(t)\right], \end{aligned} \tag{2.12}$$

where $r_j = (j-0.5)\Delta r$ is the electron radial coordinate, and the coefficients c_j and d_j are defined by

$$c_j = \frac{j^2}{j^2-\frac{1}{4}}, \quad d_j = \frac{j^2-j+\frac{1}{2}}{j^2-j+\frac{1}{4}}. \tag{2.13}$$

The discretized radial wave function $R_{j,\ell}$ is calculated on radial box of 1500 a.u. in size with a spatial step $\Delta r = 0.1$ a.u. The initial radial state $R_{j,1s}$ is generated by the inverse power method [17].

The propagation over time of the wave function is assured by split-operator method [15]:

$$R_{j,\ell}^{k+1}(t+\Delta t) = \left[I + i\tfrac{\Delta t}{2}H_0\right]^{-1}\left[I + i\tfrac{\Delta t}{2}H_{int}\right]^{-1}\left[I - i\tfrac{\Delta t}{2}H_{int}\right]\left[I - i\tfrac{\Delta t}{2}H_0\right]R_{j,\ell}^k(t), \tag{2.14}$$

where I is the unit matrix and Δt is the temporal step.

The photoelectron spectra were determined with spectral analysis of the atomic wave function, as obtained immediately after the pulse end.

In order to avoid the explicit calculation of all the eigenstates of the system, a window operator $\hat{W}(E_k, q, \gamma)$ is defined as [18, 19]

$$\hat{W}(E_k, q, \gamma) = \frac{\gamma^{2q}}{(H_0 - E_k)^{2q} + \gamma^{2q}}\ , \tag{2.15}$$

where E_k is the energy of the extracted wave function, γ is the energy width, and q is the order of the window operator.

By using the window operator in Eq. (2.15), the total probability of finding the energy of the photoelectron within the interval $E_k \pm \gamma$ at the end of the laser pulse is given by

$$\begin{aligned} P(E_k, q, \gamma) &= \langle \psi_f | \frac{\gamma^{2^q}}{(H_0 - E_k)^{2^q} + \gamma^{2^q}} | \psi_f \rangle \\ &= < \chi | \chi > \end{aligned} \tag{2.16}$$

with

$$|\chi\rangle = \frac{\gamma^{2^{q-1}}}{(H_0 - E_k)^{2^{q-1}} + i\gamma^{2^{q-1}}} |\psi_f\rangle, \tag{2.17}$$

where γ and q are parameters chosen to allow flexibility in the resolution and accuracy of the energy analysis. In the present implementation, $q = 2$ and $\gamma = 10^{-3}$ a.u.

2.2. Kroll and Watson approach

In order to test the reliability of the method that we have exploited, we propose to compare our results obtained by the spectral analysis of the wave function, which are calculated numerically by the resolution of the TDSE, with those obtained by a theoretical semiclassical treatment provided by Kroll and Watson for calculating the differential cross-section of the electron scattering process in the presence of a laser field. According to Kroll and Watson, the differential cross-section for the collision process accompanied by the exchange of n photons $(n = 1, 2, 3, ...)$ is related to the differential cross-section in the absence of the laser field $\frac{d\sigma^0}{d\theta}$ by the following formula [16]:

$$\left(\frac{d\sigma^{(n)}}{d\theta}\right)_{E_{k_0}} = \frac{k_n}{k_0} J_n^2(\alpha_0.k_n) \left(\frac{d\sigma^{(0)}}{d\theta}\right)_{E_{k_0}}\ , \tag{2.18}$$

where $k_0 = \sqrt{2(\omega_{H_{15}} - I_p)}$ is the ejected electron wave vector in the absence of the IR laser field and $k_n = \sqrt{2(\omega_{H_{15}} \pm n\omega_{IR} - I_p)}$ $(n = 1, 2, 3, ...)$ denotes its wave vector in the presence of the IR laser after exchanging n IR-photons, where $\omega_{H_{15}}$ is the energy of the harmonic photon. J_n are the ordinary Bessel functions and $\alpha_0 = \frac{E_{IR}}{\omega_{IR}^2}$ is the constant quiver radius of the free electron in the dressing IR laser. It should be noted that the KWA is a simple and convenient approximation obtained for multiphoton energy-transfer processes that accompany the scattering of a charged particle by a scattering potential in the presence of an external laser field. It is expressed in terms of the differential elastic-scattering cross-section combined with

known Bessel functions. This approach is valid when the scattering potential is weak or when the laser frequency is small. We used this approach as an ansatz for the case of a two-color photoionization process.

In order to calculate the ionization differential cross-section by a harmonic photon, i.e. in the absence of the laser field, it is sufficient to calculate the transition amplitude of the photoionization matrix element, between the initial bound state $|\psi(1s)>$ of hydrogen and its final continuum state $|\psi_{ck_0}>$ indexed by the kinetic energy $E_{k_0}=\frac{k_0^2}{2}=\omega_{H_{15}}-I_p$. Thus, the ionization differential cross-section reads

$$\begin{aligned}\left(\frac{d\sigma^{(0)}}{d\theta}\right)_{E_{k_0}} &= \left|\langle\psi_{ck_0}|\vec{\varepsilon}_{H_{15}}.\vec{r}|\psi_{1s}\rangle\right|^2 \\ &= \left|\int dr^3\psi^*_{ck_0}(\hat{r})\ \vec{\varepsilon}_{H_{15}}.\vec{r}\ \psi_{1s}(\hat{r})\right|^2.\end{aligned} \tag{2.19}$$

$\vec{\varepsilon}_{H_{15}}$ is the polarization vector of the harmonic photon.

The total cross-section is then written as follows:

$$\sigma^{(n)}=\frac{k_n}{k_0}\left|S(k_0)\right|\int_0^{\pi} sin\theta\ d\theta\ J_n^2\left(\vec{\alpha_0}.\vec{k}\right)cos^2\theta \tag{2.20}$$

with

$$S(k_0)=8\sqrt{2}\frac{1}{\sqrt{k_0(1-e^{-2\pi/k_0})}}\frac{e^{-\frac{2}{k_0}arctan(k_0)}}{(1+k_0^2)^{5/2}}. \tag{2.21}$$

3. Results and discussion

The intensity of the harmonic laser is chosen to ionize the hydrogen atom by absorption of a single photon of the 15th harmonic of the infrared laser of Ti:sapphire ($\omega_{IR}=0.057u.a.$). Subsequently, the kinetic energy $E_{H_{15}}$ of the ejected electron is simply given by

$$E_{H_{15}}=15\omega_{IR}-I_p=0.355\ a.u. \tag{3.1}$$

In Figure 1, in the absence of a laser field we observe a single photoelectron peak (blue curve) located at energy $E_{H_{15}}=0.355$ a.u.

In the case of two-color photoionization, the photoelectron spectrum consists of a principal peak related to the absorption of a harmonic photon accompanied by lateral peaks named $SB_{\pm n}$, placed symmetrically on each side (red curve). These separated satellite peaks of the same quantity, $\Delta E=\omega_{IR}$, are associated with the additional exchange of photons of the IR laser by absorption and/or stimulated emission processes.

The photoelectron peaks are shifted from their positions evaluated by Eq. (3.1) of an order of 10^{-3} a.u. This is due to Stark effect, where the energy levels are shifted by an energy quantity given by the ponderomotive energy U_p related to the infrared laser:

$$U_P=\frac{I_{IR}(W/cm^2)}{\omega_{IR}^2(a.u.)I_0(W/cm^2)}, \tag{3.2}$$

with $I_0(W/cm^2)=14.0379\times10^{16}W/cm^2$.

The kinetic energy of the ionized electron can be written as follows:

$$E_c = \omega_{H_{15}} - (I_P + U_p), \tag{3.3}$$

and the kinetic energy of satellite peaks is

$$E_{IR} = \omega_{H_{15}} \pm n\omega_{IR} - (I_P + U_P). \tag{3.4}$$

In Figure 2, we present the ATI spectra for various infrared laser intensities with a harmonic laser intensity fixed to $I_{H_{15}} = 10^9$ W/cm^2. By increasing the infrared intensity I_{IR}, the probability of the satellite peaks increases while the probability related to the harmonic peak decreases, and the birth of other satellite peaks is possible as well. The phenomenon is seen as if the probability of the harmonic peak was partly transformed into satellite peaks.

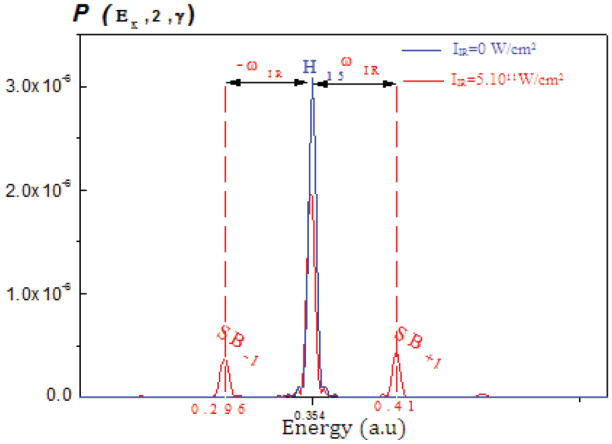

Figure 1. Photoelectron energy spectrum obtained by photoionization of hydrogen by the Ti:sapphire laser of fundamental frequency $\omega_{H_{15}} = 0.855$ a.u. combined with its 15th harmonics for a harmonic intensity $I_{H_{15}} = 10^9$ W/cm^2 and different laser intensities $I_{IR} = 0$ W/cm^2 (single-photon ionization) (blue curve) and $I_{IR} = 5 \times 10^{11}$ W/ cm^2 (red curve).

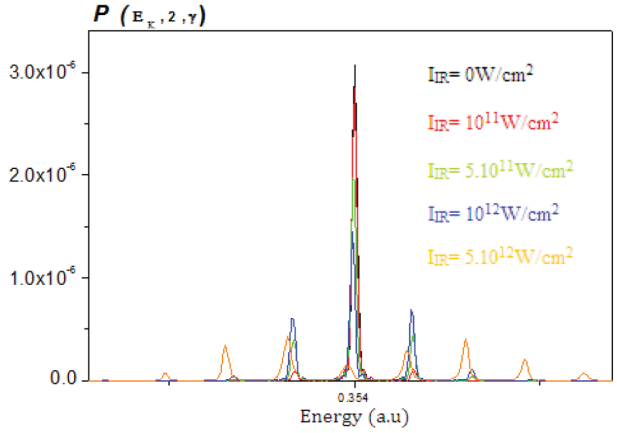

Figure 2. Photoelectron energy spectrum obtained by photoionization of hydrogen by the Ti:sapphire laser of fundamental frequency $\omega_{IR} = 0.057$ a.u. combined with its 15th harmonics $\omega_{H_{15}} = 0.855$ a.u. for a harmonic intensity $I_{H_{15}} = 10^9$ W/cm^2 and different laser intensities.

As we have already explained, in Figure 3, in addition to the peak associated with the ionization of hydrogen by the absorption of a harmonic photon of frequency $\omega_{H_{15}}$, two satellite peaks named SB_{+1} and SB_{-1}, separated by $2\omega_{IR}$, appear on the spectrum. These two peaks correspond to the absorption and emission of a single photon infrared. As we see in Figure 3, there is good agreement between the spectrum obtained with the TDSE results (black curve) and those obtained by the KWA approximation (red curve).

In order not to be limited by the ionization threshold, it is necessary to increase the energy of the harmonic photon responsible for the ionization of hydrogen in the presence of the infrared laser field, which makes it possible to have more satellite peaks on the spectrum, i.e. to have a greater exchange of infrared photons.

We choose to take, for example, the 41st harmonic of a Ti:sapphire laser, but this can pose a problem of reflection on the boundaries of the simulation box, because the ejected electron will move much more rapidly in the continuum due to the large value of kinetic energy acquired from the harmonic field and the risk would be to have a problem in the convergence of numerical results. Consequently, it is necessary to increase the size of the simulation box to avoid this problem of reflection.

3.1. Convergence of TDSE results

Several criteria are possible to verify the convergence of the results. Among these, we retain the evolution of the norm of the wave function over time, $N_{\ell_{max}}(t) = \sum_{r=0}^{R_{max}} \left|\psi_{\ell_{max}}(r,t)\right|^2 \Delta r$, for some maximum values of the angular momentum of the free electron ℓ_{max}.

The convergence criterion is verified to a decrease of the norm $N_{\ell_{max}}(t)$ when the value of maximum angular momentum increases; this is clearly observed in Figure 4. For example, if we take the case of a high value of ℓ_{max}, a decrease of the order of $\sim 10^{-10}$ is seen in Figure 4, i.e. $N_{90} \ll \frac{N_1}{10^5}$, and this allowed us to ensure the convergence of our program and the results obtained.

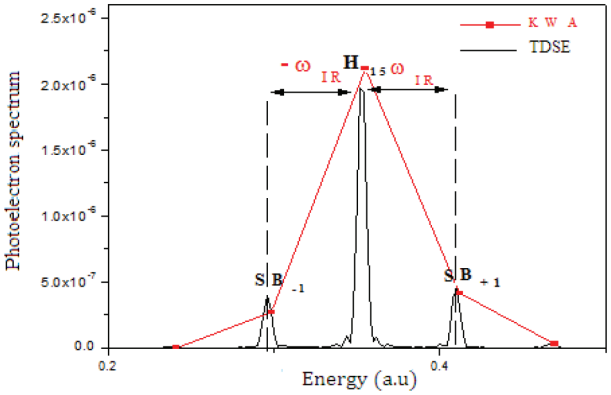

Figure 3. Comparison of photoelectron spectra obtained by solving the TDSE and those obtained by KWA for a hydrogen atom interacting with a linearly polarized infrared laser field of intensity $I_{IR} = 5 \times 10^{11}$ W/cm^2 combined with its 15th harmonic of intensity $I_{H_{15}} = 10^9$ W/cm^2.

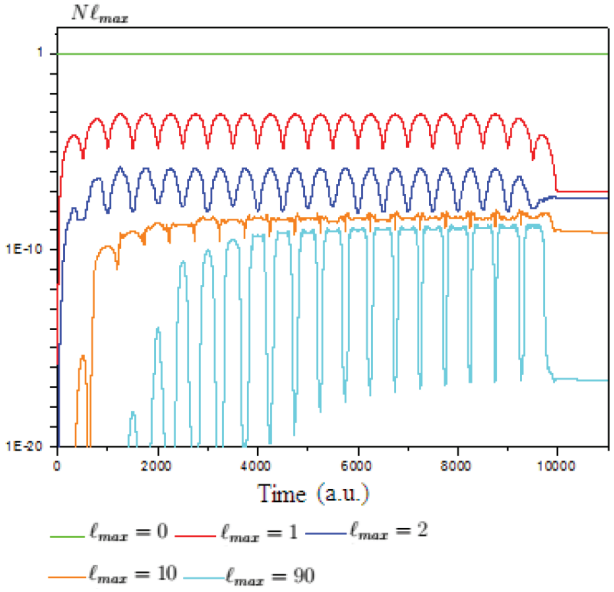

Figure 4. Temporal evolution of the norm of the wave function with different L_{max} values.

After confirming the convergence of the results, we compare the energy spectrum of the ejected electron obtained by calculating the probability $P(E_k, n, \gamma)$ from the numerical solution of the TDSE with the spectrum obtained by calculating the differential cross-section using the KWA. The two spectra are shown in Figure 5 for laser intensities of 5×10^{11} W/cm^2 and 5×10^{12} W/cm^2. We choose the last intensity in order to increase the number of satellite peaks as much as possible. From this figure we can say that qualitatively there is good agreement between the two spectra, but they are a little different quantitatively, which ensures the reliability of the numerical methods used for the resolution of the TDSE. Indeed, the number of satellite peaks is identical and also their intensities, even if some variations on the order of 10% are observed between the approximation and the exact calculation. It should be noted that the KWA is much less demanding in terms of computational power than the resolution of the TDSE. In addition, we obtain interesting results concerning the relative importance of the contributions of the Born terms as compared with the above-mentioned sophisticed numerical treatment.

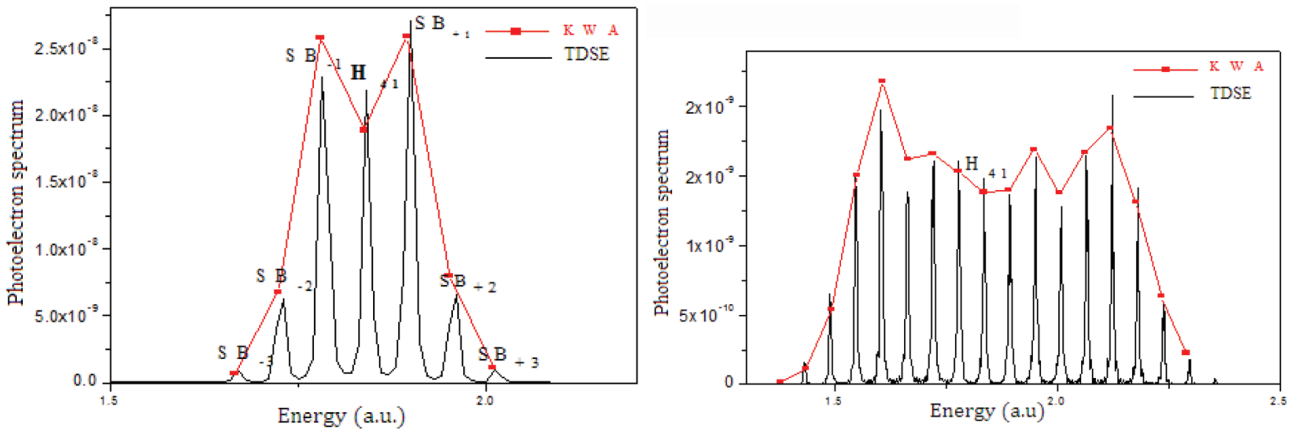

Figure 5. Comparison of photoelectron spectra obtained by solving the TDSE and those obtained by KWA for a hydrogen atom interacting with a linearly polarized infrared laser field of intensity a) $I_{IR} = 5 \times 10^{11}$ W/cm^2 and b) $I_{IR} = 5 \times 10^{12}$ W/cm^2 combined with its 41st harmonic of intensity $I_{IR} = 5 \times 10^{12}$ W/cm^2.

4. Conclusion

We have presented a set of results obtained by numerical solution of the three-dimensional time-dependent Schrödinger equation. We have discussed the case of processes that can take place in the simultaneous presence of the fundamental of an IR laser and its 15th harmonic with a frequency large enough to ionize the hydrogen atom by single-photon absorption. To check the validity of our results, we have compared the obtained two-color spectra through direct solution of the TDSE with those obtained using the KWA. This comparison shows good agreement between the two methods. We can therefore conclude that the methods employed in the resolution of the TDSE are very useful in describing the two-color ionization process of hydrogen. This work was devoted mainly to the ATI spectra of two-color photoionization. The scattering of the freed electron assisted by infrared radiation is behind the phenomena of absorption and emission of infrared photons. In a future work, we will give more attention to this scattering problem.

Acknowledgment

The authors would like to thank the anonymous reviewers for their constructive comments and contributions to this study.

References

[1] Hall, J. L.; Robinson, E. J.; Branscomb, L. M. *Phys. Rev. Lett.* **1965**, *14*, 1013-1017.

[2] Keldysh, L. V. *Sov. Phys. JETP* **1965**, *20*, 1307-1317.

[3] Agostini, P.; Fabre, F.; Mainfray, G.; Petite, G.; Rahman, N. K. *Phys. Rev. Lett.* **1979**, *42*, 1127-1130.

[4] Yuan-Yuan, N.; Song-Feng, Z.; Xiao-Yong, L.; Guo-Li, W.; Xiao-Xin, Z. *Chin. Phys. B* **2018**, *27*, 073203.

[5] Shore, B. W.; Knight, P. L. *J. Phys. B* **1987**, *20*, 413-423.

[6] L'Hullier, A.; Balcou, P. *Phys. Rev. Lett.* **1993**, *70*, 774-777.

[7] Suárez, N.; Chacón, A.; Pérez-Hernández, J. A.; Biegert, J.; Lewenstein, M.; Ciappina, M. F. *Phys. Rev. A* **2017**, *95*, 033415

[8] Benis, E. P.; Charalambidis, D.; Kitsopoulos, T. N.; Tsakiris, G. D.; Tzallas, P. *Phys. Rev. A* **2006**, *74*, 051402.

[9] Meyer, M.; Costello, J. T.; Düsterer, S.; Li, W. B.; Radcliffe, P. *J. Phys. B* **2010**, *43*, 194006.

[10] Bottcher, M.; Rottke, H.; Zhavoronkov, N.; Sandner, W.; Agostini, P.; Gisselbrecht, M.; Huetz, A. *Phys. Rev. A* **2007**, *75*, 033408.

[11] Mancuso, C. A.; Hickstein, D. D.; Grychtol, P.; Knut, R.; Kfir, O.; Xiao-Min, T.; Dollar, F.; Zusin, D.; Gopalakrishnan, M.; Gentry, C. et al. *Phys. Rev. A* **2015**, *91*, 031402(R).

[12] Ivanov, I. A.; Kheifets, A. S. *Phys. Rev. A* **2017**, *96*, 013408.

[13] Kulander, K. C. *Phys. Rev. A* **1987**, *35*, 445-447.

[14] Varga, R. S. *Matrix Iterative Analysis*; Prentice Hall: New York, NY, USA, 1962.

[15] Kroll, N. M.; Watson, K. M. *Phys. Rev. A* **1973**, *8*, 804-809.

[16] Chqondi, S.; Taïeb, R.; Makhoute, A. *International Journal of Innovation and Applied Studies* **2014**, *6*, 504-514.

[17] Press, W. H.; Teukolsky, S. A.; Vetterling, W. T.; Flannery, B. P. *Numerical Recipes, 3rd Edition: The Art of Scientific Computing*; Cambridge University Press: New York, NY, USA, 2007.

[18] Schafer, K. J. *Computer Physics Communications* **1991**, *63*, 427-434.

[19] Chang-Ping, S.; Song-Feng, Z.; Jian-Hong, C.; Xiao-Xin, Z. *Chin. Phys. B* **2011**, *20*, 113201.